

## Article

# Process Assessment of Integrated Hydrogen Production from By-Products of Cottonseed Oil-Based Biodiesel as a Circular Economy Approach

Dhyna Analyses Trirahayu <sup>1,\*</sup>, Akhmad Zainal Abidin <sup>2,\*</sup>, Ridwan P. Putra <sup>2</sup>, Firda Dwita Putri <sup>3</sup>, Achmad Syarif Hidayat <sup>4</sup> and Muhammad Iqbal Perdana <sup>5</sup>

<sup>1</sup> Department of Chemical Engineering, Politeknik Negeri Bandung, Jalan Geger Kalong Hilir, Bandung 40012, Indonesia

<sup>2</sup> Department of Chemical Engineering, Faculty of Industrial Technology, Institut Teknologi Bandung, Jalan Ganesha 10, Bandung 40132, Indonesia; ridwan@masaroitb.com

<sup>3</sup> Department of Chemical Engineering, Faculty of Engineering, Universitas Sebelas Maret, Jalan Ir. Sutami 36A, Surakarta 57126, Indonesia

<sup>4</sup> Research and Analytical Center for Giant Molecules Section of Analysis Research, Graduate School of Science, Tohoku University, 2-1-1 Katahira, Aoba-ku, Sendai 980-8577, Japan

<sup>5</sup> Department of Science, Faculty of Science and Technology, Prince of Songkla University Pattani Campus, Pattani 94000, Thailand

\* Correspondence: dhyna.analyses@polban.ac.id (D.A.T.); zainal@che.itb.ac.id (A.Z.A.)

**Abstract:** Cottonseed oil (CSO) is well known as one of the commercial cooking oils. However, CSO still needs to compete with other edible oils available in the market due to its small production scale and high processing cost, which makes it a potential candidate as a feedstock for biodiesel production. To date, transesterification is the most widely applied technique in the conversion of vegetable oil to biodiesel, with glycerol produced as a by-product. Large-scale biodiesel production also implies that more glycerol will be produced, which can be further utilized to synthesize hydrogen via the steam reforming route. Therefore here, an integrated biodiesel and hydrogen production from CSO was simulated using Aspen Hysys v11. Simulation results showed that the produced biodiesel has good characteristics compared to standard biodiesel. An optimum steam-to-glycerol ratio for hydrogen production was found to be 4.5, with higher reaction temperatures up to 750 °C resulting in higher hydrogen yield and selectivity. In addition, a simple economic analysis of this study showed that the integrated process is economically viable.

**Keywords:** biodiesel; cottonseed oil; hydrogen; process simulation; steam reforming; transesterification



**Citation:** Trirahayu, D.A.; Abidin, A.Z.; Putra, R.P.; Putri, F.D.; Hidayat, A.S.; Perdana, M.I. Process Assessment of Integrated Hydrogen Production from By-Products of Cottonseed Oil-Based Biodiesel as a Circular Economy Approach. *Hydrogen* **2023**, *4*, 272–286. <https://doi.org/10.3390/hydrogen4020019>

Academic Editors: Eugenio Meloni, Marco Martino and Concetta Ruocco

Received: 2 April 2023

Revised: 29 April 2023

Accepted: 5 May 2023

Published: 8 May 2023



**Copyright:** © 2023 by the authors. Licensee MDPI, Basel, Switzerland. This article is an open access article distributed under the terms and conditions of the Creative Commons Attribution (CC BY) license (<https://creativecommons.org/licenses/by/4.0/>).

## 1. Introduction

Energy demands and consumption have been increasing with rapid population and industrial sector growth. Fossil fuels are considered the primary energy source, even though they are limited in resources and have negative impacts on the environment. Nevertheless, fossil fuels may contain many harmful substances that can induce various environmental issues, e.g., global warming, air pollution, acid rain, and ozone layer depletion, which can negatively influence human health [1]. Numerous studies have been conducted in hopes of finding alternative fuels that can replace fossil fuels. In addition, it is also very important for the fuel resources to be economically viable, environmentally safe, and available in abundant quantities at a low cost. Among the accessible resources, biodiesel is considered a promising alternative that can be used to replace diesel oil and other petroleum-based fuels [2].

Biodiesel can be produced from renewable sources that deem it safe, biodegradable, harmless, sulphur-free, and considered an effective lubricant [3]. The advantages of biodiesel compared to fossil fuels cannot be overstated. The commercialization of biodiesel

as a fuel can be carried out by blending it with diesel oil or using it directly as a pure substance. It is also highly compatible with diesel engines, requiring no further modifications or causing undesirable effects on engine performance [4]. Biodiesel can be generated from a wide range of biomass, including vegetable oils [5], animal fats [6], microbial lipids [7], and waste cooking oil [8], which are accessible and renewable. Many varieties of vegetable oil have been explored as biodiesel feedstocks that can be categorized into edible oil and non-edible oil groups. To date, the majority of commercial biodiesel is produced from edible oils, including cottonseed oil (CSO) [9,10].

The development of biodiesel production starts at a laboratory scale, and scaling up the process is a major challenge. Process simulation can be used to model, predict, and optimize the process in a more economical way. Therefore, process simulation can be employed as an inexpensive tool to scale up for design considerations, production estimations, and product property assessments. In previous studies, we have actively simulated various processes associated with the utilization of vegetable oils as raw materials for biodiesel or other value-added products [11–15]. The production of biodiesel from a variety of feedstock can be accomplished by four main pathways: direct use and blending, microemulsion, pyrolysis, as well as transesterification. Among the four methods stated, transesterification is the most widely applied in biodiesel production. Here, the triglycerides are reacted with an alcohol, most preferably methanol, in the presence of a catalyst, transforming them into fatty acid methyl esters (FAMES) or biodiesel and glycerol as by-products [16].

Glycerol can be transformed into various products via many different routes, either chemical or biochemical. In particular, value-added products, such as hydrogen, acrolein, glycerol carbonate, dihydroxyacetone, glyceric acid, propylene glycol, benzoic acid, and other value-added products can be obtained [17]. Among all these products, hydrogen is one of the most promising renewable energies that can be produced through an integrated process with biodiesel production. Glycerol is considered an attractive feedstock for hydrogen production and power generation, as the yields obtained from biodiesel production can meet its demand in the market [18–20]. The catalytic reforming of glycerol for the production of hydrogen and other energy carriers/chemicals is achieved via glycerol dehydrogenation on the catalytically active side, followed by water–gas shift or methanation reactions.

Therefore, in this work, ASPEN Hysys v11 was used to model and simulate an integrated process of CSO transesterification for biodiesel production and glycerol steam reforming to produce hydrogen. The simulation focused on the properties of the biodiesel products, which are further evaluated using the available criteria, and the effect of operating conditions on hydrogen production. To the best of our knowledge, there are no studies that report the simulation process of integrated CSO transesterification for biodiesel production and glycerol steam reforming to produce hydrogen.

## 2. Process Simulation

### 2.1. Biodiesel Production from Cottonseed Oil

CSO is one of the commercial cooking oils that gradually loses market share to other vegetable oils with higher production and lower costs, such as palm oil, which dominates the Indonesian market. However, with regard to active research on biodiesel production from vegetable oils, CSO as a feedstock for biodiesel production is prospective and may have the potential to increase the viability of the cottonseed industry [21]. The physical properties of CSO and the fatty acid contents of CSO are summarized in Tables 1 and 2, respectively. These values were used to carry out the simulation in this study.

**Table 1.** Physical properties of cottonseed oil [22,23].

Property	Value
Acid value	1.11 mg KOH/L of oil
Saponification value	186.175–199.7 mg KOH/g of oil
Density	0.875–0.905 g/cc
Iodine value	98.4–107 g of iodine/100 g oil

**Table 2.** Fatty acid compositions present in cottonseed oil [22,24,25].

Fatty Acid	% Composition
Myristic acid	0.8–1.0
Palmitic acid	19.78–24.4
Palmitoleic acid	0.4–0.6
Stearic acid	1.57–3.4
Oleic acid	15.59–19.4
Linoleic acid	53.2–55.0
Linolenic acid	0.3–0.5

### 2.1.1. Esterification Process

CSO may have high FFA concentrations, depending on the quality of the oil. CSO feedstocks containing more than 1% FFA need to be esterified to eliminate the negative effects of saponification, which can reduce biodiesel yield as the oil is converted to soap. To remove water and other contaminants, CSO, as the raw material, needs to be filtered and pretreated so that the performance of the process is improved. In the esterification process, the FFA content in CSO is reacted with alcohol, preferably methanol, in the presence of an acid catalyst and then converted to biodiesel and water in the reactor. Traditionally, a homogeneous catalyst with an acidic property, commonly sulfuric acid, is used in the esterification process. As the catalyst is homogenous, it can be mixed with the pretreated oil after being dispersed in methanol. Subsequently, FFA-depleted biodiesel is produced, and the mixture is heated and stirred in the reactor at optimum reaction conditions. Water is then removed after the reaction conversion is achieved. The consumed FFA makes the stream proceed to the transesterification reaction. Acidic catalysts are not easy to implement due to their corrosive characteristics, neutralization issues, and the need for extensive waste disposal, making it difficult to use a strong acid as a catalyst. Many studies have explored other alternatives to strong acid catalysts to address these shortcomings, such as heterogeneous catalysts derived from sulfonated carbonaceous materials [26] or silica zirconia [27]. Equation (1) describes a typical biodiesel reaction resulting from an acid-catalyzed esterification reaction.



### 2.1.2. Transesterification Process

Transesterification is the most commonly applied method for converting vegetable oil into biodiesel and glycerol. Biodiesel and glycerol are produced when triglycerides in vegetable oils react with alcohols in the presence of alkaline catalysts. As mentioned earlier, the oil feedstock should contain less than 1% FFA for the transesterification reaction to proceed efficiently. Raw materials must be pretreated to separate water and other contaminants before being fed directly into the transesterification reactor, making the reactor inlet contain triglycerides and fatty acid alkyl esters produced from the esterification process. The most common catalyst used in transesterification reactions is NaOH in aqueous form, so it can be mixed directly with the feed stream as it enters the reactor [28]. When acid esterification reactions are involved, additional base catalysts may be required to neutralize the acid. The biodiesel and glycerol produced form two liquid layers as the reaction proceeds. In general, transesterification reactions are usually carried out at low reaction

temperatures (60–70 °C) and pressures (atmospheric pressure). The presence of a catalyst in the transesterification process is essential to ensure that the reaction proceeds to biodiesel production. Homogeneous catalysts require extra work for separation purposes, making a heterogeneous catalyst an interesting choice. Metal-oxide-based heterogeneous catalysts have been intensively studied for their application as catalysts in transesterification reactions to generate biodiesel [29,30]. Environmentally friendly alternatives, such as calcium oxides from calcium-rich natural resources such as eggshells [31,32], cockle shells [33], or other animal shells, can also serve as catalysts. General biodiesel production via an alkali-catalyzed esterification reaction is stated in Equation (2).

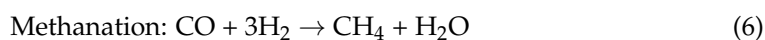
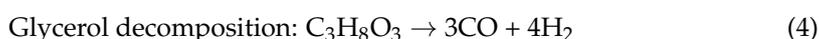
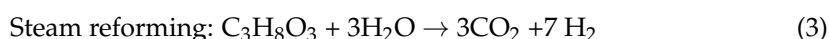


### 2.1.3. Biodiesel Purification

To ensure the conversion of CSO to biodiesel, the transesterification reaction is performed in a methanol-rich environment. Methanol remaining in the product stream must be removed for economic reasons. In addition to unreacted methanol, the side products, including water and glycerol, must be separated from the biodiesel product stream to meet the biodiesel standards. Wet scrubbing, dry scrubbing (activated compounds, biomass-based adsorbents, and silica-based adsorbents), ion exchange, or membrane separation technology are all options for biodiesel refining [34]. The purity of biodiesel that needs to be achieved is the determining factor in selecting the appropriate technology. Membrane technology may be a viable option for separating glycerol from biodiesel, but special efforts are necessary to prevent membrane fouling and clogging [34]. Other emerging technologies, such as high-voltage electrolysis, may be good candidates for separating glycerol from biodiesel [35]. Distillation has traditionally been used to separate and recover methanol [36]. Recently, the use of membrane reactors has become popular because of their advantages in enhancing the purification process [37].

### 2.2. Glycerol Steam Reforming to Produce Hydrogen

Hydrogen production from glycerol can be achieved via various routes. Steam reforming is the most common reaction for this application. The reaction pathway to produce hydrogen from glycerol involves complex reactions, which are summarized in Equations (3)–(6).



The first three reactions increase the hydrogen yield of the production process, while the fourth (methanation) reduces the hydrogen yield because the hydrogen produced is consumed as a reactant. However, this process is known to improve the heat balance [18].

As the key parameters to evaluate the process, glycerol conversion, hydrogen yield, and hydrogen selectivity are described in Equations (7)–(10).

$$\text{Glycerol conversion : } x_{\text{glycerol}} = \frac{n \text{ Glycerol}_{\text{in}} - n \text{ Glycerol}_{\text{out}}}{n \text{ Glycerol}_{\text{in}}} \times 100\% \quad (7)$$

$$\text{CO CO}_2 \text{ CH}_4 \text{ Yield : } Y_{\text{CO,CO}_2, \text{CH}_4} = \frac{\text{mole fraction of CO, CO}_2, \text{CH}_4 \text{ in product}}{\text{Total C atoms in feedstock}} \times 100\% \quad (8)$$

$$\text{Hydrogen Yield : } Y_{\text{H}_2} = \frac{\text{moles H}_2 \text{ in product}}{\text{moles Glyceron in feedstock} \times 7} \times 100\% \quad (9)$$

$$\text{Hydrogen Selectivity : } S_{\text{H}_2} = \frac{\text{moles H}_2 \text{ in product}}{\text{moles CO, CO}_2, \text{CH}_4 \text{ in product}} \times \frac{1}{\text{RR}} \times 100\% \quad (10)$$

### 2.3. Simulation Methodology

All processes were simulated using Aspen Hysys v11 with the following assumptions. The raw materials for biodiesel production used in this study were CSO with a basis of 1000 kg/h and methanol. Due to the high FFA composition of CSO (>1%), the biodiesel production process involves esterification and transesterification. Glycerol as a by-product was then converted to hydrogen via a steam reforming process, followed by a water–gas shift reaction to eliminate carbon monoxide. The triglyceride compositions in CSO were simplified by using the major fatty acids in CSO, including triolein, tristearin, trilinolein, and tripalmitin. Trilinolein and tripalmitin are expressed using hypothetical components to better imitate the characteristics of CSO, while oleic acid is employed to represent the FFA composition. The simulation parameters for the integrated process of biodiesel production are summarized in Table 3, and the simulation parameters for hydrogen production are stated in Table 4.

**Table 3.** Cottonseed oil to biodiesel simulation parameters.

Parameter	Value
CSO flowrates (kg/h)	1000
Methanol-to-oil ratio	6:1
Reaction temperature (°C)	65
Conversion (%)	100
CSO compositions (%-mole)	
Triolein	13.08
Trilinolein	42.31
Tripalmitin	20.31
Tristearin	1.86
Oleic acid (FFA)	22.43

**Table 4.** Glycerol steam reforming for hydrogen production simulation parameters.

Parameters	Values
Steam-to-glycerol molar ratio	0.5–10
Reaction temperature (°C)	400–750

## 3. Results and Discussion

### 3.1. Biodiesel Production from Cottonseed Oil

Figure 1 depicts the simulation flowsheet for the biodiesel production process from cottonseed oil. Esterification, transesterification, and biodiesel purification are all part of the process. Major key equipment is used in the simulation, involving reactors, process separation units, heat exchangers, and pumps. Table 5 summarizes codes and descriptions for each piece of process equipment.

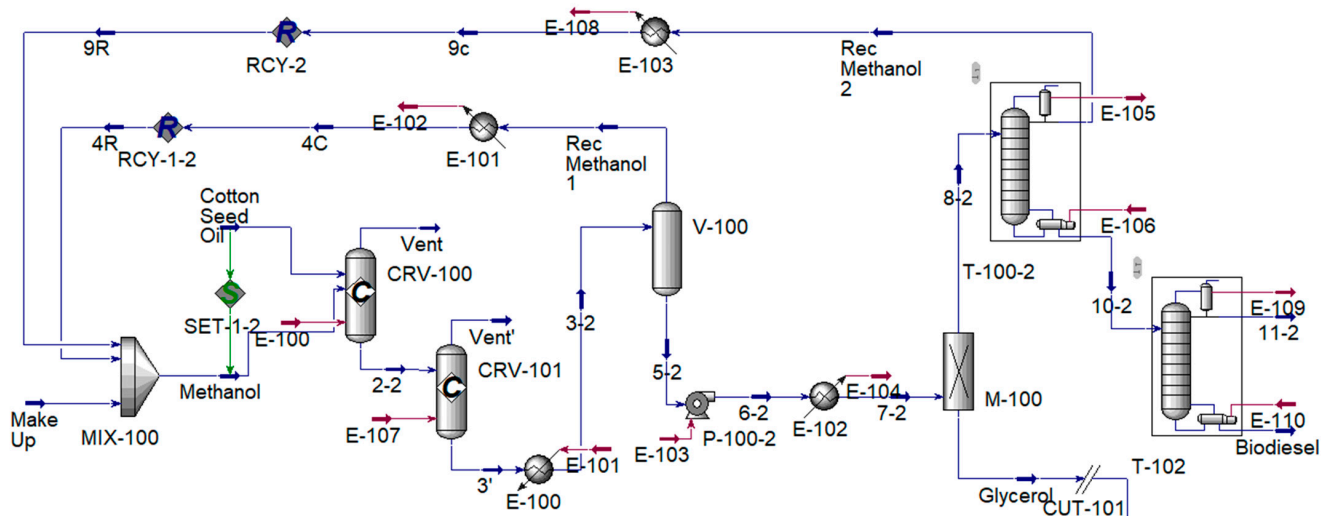


Figure 1. Biodiesel production from CSO simulation flowsheet using Aspen Hysys v11.

Table 5. Equipment description of the cottonseed oil to biodiesel simulation flowsheet using Aspen Hysys v11.

Code	Description
MIX-100	Methanol mixer
CRV-100	Esterification reactor
CRV-101	Transesterification reactor
V-100	Flash distillation column
M-100	Membrane
T-100 and T-102	Fractional distillation column
P-100	Membrane pump
E-100, E-101, E-102, and E-103	Heat exchanger

The process reactor inlets were CSO (1000 kg/h) as an oil feedstock and methanol as an alcohol source, with a methanol-to-oil ratio of 6:1. The CSO stream was simulated with a composition of triolein (13.08%), trilinolein (42.31%), tripalmitin (20.31%), tristearin (1.86%), and oleic acid (22.43%) as FFA. Since CSO contains more than 1% FFA, it needs to be esterified first before proceeding with the transesterification reaction. Because of data constraints, both the esterification and transesterification reactions were modeled by conversion reactors. The conversion for both processes (esterification and transesterification) was set at 100%.

Temperature is another factor that influences biodiesel yield. According to the literature review, both reactors can be operated at the same operating conditions (65 °C, atmospheric pressure). Most of the remaining methanol, water, glycerol, and biodiesel were found in the output stream of the second reactor. Biodiesel was used as a fuel, which is required to meet the standards available, especially the qualification from the purity level. Excess methanol must be recovered for economic efficiency. The product was then processed through a series of separation steps for methanol recovery, glycerol separation, and biodiesel purification to produce high-quality biodiesel.

Two stages of separation were utilized to maximize the methanol recovery: flash distillation and fractional distillation. Flash distillation requires the outlet of the transesterification process reactor to be heated to 80 °C in a flash drum to form a vapor–liquid mixture. This mixture contains a methanol fraction enriched in the vapor phase and can be used to remove most of the excess methanol. The methanol-rich vapor phase was then cooled down and used as feed. Most of the unreacted methanol was recovered using this method, with a recovery of approximately 65%.

The liquid stream then proceeded to the next stage, which was the glycerol separation. The operation could be carried out using a variety of technologies [34]. Considering many aspects, membrane separation may be the best candidate for this purpose due to its selectivity and rejection rate for specific components [38,39]. Because the high retention of the membrane results in optimal process conditions, membrane separation needs to be performed at high pressure (5.5 bar) and low temperature (25 °C) to protect the membrane material. The residue was 99% glycerol (97.54 kg/h) together with other impurities. The rich biodiesel permeate stream was sent to a fractional distillation column (T-100) for biodiesel refining. About 30% of the excess methanol could be recovered after the fractional distillation process, bringing the total amount of recycled methanol up to 95%. After a series of purification steps, the biodiesel had an ester composition of up to 99.97% at a mass flow rate of 1008 kg/h. The detailed mass and energy balances for each stream are summarized in Table 6.

**Table 6.** Mass and energy balances for biodiesel production.

Stream	9R	4R	Make Up	Methanol	CSO	2-2	3'	3-2	R Methanol 1
Vapor fraction	0.0000	0.0000	0.0000	0.0000	0.0000	0.0000	0.0000	0.0727	1.0000
Temperature (°C)	25	25	25	25	25	65	65	85	85
Pressure (kPa)	100	100	100	100	100	100	100	100	100
Molar flow (kgmole/h)	3.98	0.70	3.52	8.20	1.37	9.56	9.56	9.56	0.70
Mass flow (kg/h)	126.26	22.01	112.22	260.49	1000.00	1260.50	1260.47	1260.47	21.98
Heat flow (MJ/h)	−958	−168	−844	−1970	−2063	−3913	−4169	−4089	−139
Component	Mole Fraction								
Glycerol	0.0000	0.0000	0.0000	0.0000	0.0000	0.0000	0.1108	0.1108	0.0000
H <sub>2</sub> O	0.0250	0.0308	0.0100	0.0190	0.0000	0.0484	0.0484	0.0484	0.0308
Triolein	0.0000	0.0000	0.0000	0.0000	0.1308	0.0187	0.0000	0.0000	0.0000
Trilinolein	0.0000	0.0000	0.0000	0.0000	0.4231	0.0604	0.0000	0.0000	0.0000
Tripalmitin	0.0000	0.0000	0.0000	0.0000	0.2031	0.0290	0.0000	0.0000	0.0000
Tristearin	0.0000	0.0000	0.0000	0.0000	0.0186	0.0027	0.0000	0.0000	0.0000
Oleic acid	0.0000	0.0000	0.0000	0.0000	0.2243	0.0000	0.0000	0.0000	0.0000
Methanol	0.9750	0.9692	0.9900	0.9810	0.0000	0.8088	0.4763	0.4763	0.9692
M-Oleate	0.0000	0.0000	0.0000	0.0000	0.0000	0.0320	0.0881	0.0881	0.0000
M-Linoleate	0.0000	0.0000	0.0000	0.0000	0.0000	0.0000	0.1813	0.1813	0.0000
M-Palmitate	0.0000	0.0000	0.0000	0.0000	0.0000	0.0000	0.0870	0.0870	0.0000
M-Stearate	0.0000	0.0000	0.0000	0.0000	0.0000	0.0000	0.0080	0.0080	0.0000
Stream	5-2	6-2	7-2	Glycerol	8-2	R Methanol 2	10-2	11-2	Biodiesel
Vapor fraction	0.0000	0.0000	0.0000	0.0000	0.0000	0.0000	0.0000	0.0000	0.0000
Temperature (C)	85	85	25	25	25	65	185	99	287
Pressure (kPa)	100	550	550	100	100	100	100	100	100
Molar flow (kgmole/h)	8.87	8.87	8.87	1.06	7.81	3.98	3.83	0.34	3.49
Mass flow (kg/h)	1238.49	1238.49	1238.49	97.54	1140.95	126.18	1014.77	6.29	1008.48
Heat flow (MJ/h)	−3950	−3949	−4109	−717	−3392	−940	−2096	−95	−1742
Component	Mole Fraction								
Glycerol	0.1195	0.1195	0.1195	0.9996	0.0003	0.0000	0.0006	0.0000	0.0006
H <sub>2</sub> O	0.0497	0.0497	0.0497	0.0000	0.0565	0.0250	0.0892	0.9982	0.0006
Triolein	0.0000	0.0000	0.0000	0.0000	0.0000	0.0000	0.0000	0.0000	0.0000
Trilinolein	0.0000	0.0000	0.0000	0.0000	0.0000	0.0000	0.0000	0.0000	0.0000
Tripalmitin	0.0000	0.0000	0.0000	0.0000	0.0000	0.0000	0.0000	0.0000	0.0000
Tristearin	0.0000	0.0000	0.0000	0.0000	0.0000	0.0000	0.0000	0.0000	0.0000
Oleic acid	0.0000	0.0000	0.0000	0.0000	0.0000	0.0000	0.0000	0.0000	0.0000
Methanol	0.4377	0.4377	0.4377	0.0000	0.4970	0.9750	0.0000	0.0000	0.0000
M-Oleate	0.0950	0.0950	0.0950	0.0004	0.1078	0.0000	0.2199	0.0003	0.2414
M-Linoleate	0.1956	0.1956	0.1956	0.0000	0.2220	0.0000	0.4529	0.0001	0.4971
M-Palmitate	0.0939	0.0939	0.0939	0.0000	0.1066	0.0000	0.2174	0.0013	0.2385
M-Stearate	0.0086	0.0086	0.0086	0.0000	0.0098	0.0000	0.0200	0.0000	0.0219

The biodiesel product properties obtained from the simulated process in this study were compared to experimental studies utilizing CSO as feedstock (Table 7). The properties of biodiesel modeled from the simulation process are comparable to other similar experimental studies on biodiesel production from CSO. The properties are also consistent with biodiesel standards from the literature (ASTM D 6751 and EN 14214).

**Table 7.** Biodiesel properties generated from cottonseed oil compared to standards from the literature.

Properties	ASTM D 6751 Standards	EN 14214 Standards	Alhassan et al. [40]	Augustine et al. [41]	This Study
Water and sediment, max	<0.05	<0.05	-	-	0.0036
Viscosity (cSt) @ 40 °C	1.9–6.0	3.5–5.0	4.38	7.75	2.6
Density @ 15 °C (kg/m <sup>3</sup> )	870–900	860–900	887	913	664.9
Ester content		>96.5	96.85	-	99.97

3.2. Glycerol Steam Reforming to Produce Hydrogen

Figure 2 depicts the simulation flowsheet for the hydrogen production process from glycerol. The process was modeled with two reactors, one for the steam reforming process and one for the low-temperature separation (LTS) water–gas shift reaction. The process was followed by purification processes, which include flash distillation, absorption, and distillation. The main equipment involved in the process were reactors, flash tanks, absorption columns, and distillation columns, as well as auxiliary equipment such as pumps, heat exchangers, and compressors. Table 8 summarizes the codes and descriptions for key equipment.

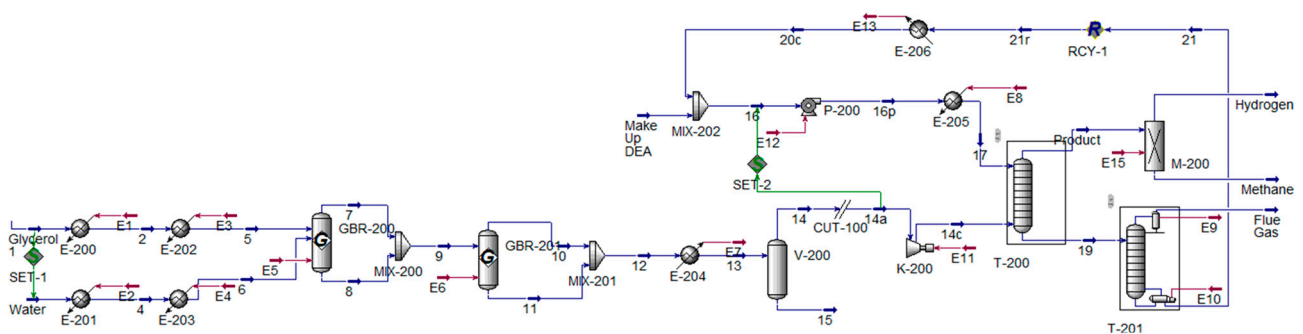


**Figure 2.** Hydrogen production from glycerol simulation flowsheet using Aspen Hysys v11.

**Table 8.** Equipment description of hydrogen production process from glycerol using Aspen Hysys v11.

Code	Description
GBR-200	Steam reforming reactor
GBR-201	Water–gas shift reactor
V-200	Flash drum
T-200	Absorption tower
T-201	Distillation tower
M-200	Membrane
K-200	Compressor
P-200	Pump
E-200, E-201, E-202, E-203, E-204, E-205, and E-206	Heat exchanger

The mass and energy balances for hydrogen production are summarized in Table 9. The glycerol stream with a mass flow rate of 97.54 kg/h separated from the biodiesel production product stream was heated to reach the reaction temperature. In addition to glycerol, the steam generated in the steam reforming process also entered the reactor GBR-200 as superheated steam. In the GBR-200 reactor, the hydrogen production process was modeled by four reactions: glycerol steam reforming, glycerol decomposition, water–gas shift reaction, and methanation reaction. To eliminate the carbon dioxide composition from the product stream, the GBR-200 product stream entering the second reactor (GBR-201) underwent a low-temperature water–gas shift reaction. The reactor was modeled with a water–gas reaction only. The output of GBR-200 was then cooled down to separate most of the water formed. The gas stream separated from water was then compressed before

entering the absorption column to separate carbon dioxide using DEA as a solvent. The gas stream leaves the absorber with a high concentration of hydrogen and a mass flow rate of 8.45 kg/h.

**Table 9.** Mass and energy balances for hydrogen production.

Stream	Glycerol	Water	5	6	9	12	13	14	14c
Vapor fraction	0.0000	0.0000	1.0000	1.0000	0.6477	1.0000	0.9398	1.0000	1.0000
Temperature (°C)	25	25	600	600	600	100	50	50	169
Pressure (kPa)	100	100	100	100	100	100	100	100	270
Molar flow (kgmole/h)	1.06	3.17	1.06	3.17	8.99	8.99	8.99	8.45	8.45
Mass flow (kg/h)	97.54	57.17	97.41	57.17	154.58	154.58	154.58	144.83	144.83
Heat flow (MJ/h)	−717	−904	−513	−698	−1188	−1356	−1394	−1241	−1207
Component	Mole Fraction								
Glycerol	1.0000	0.0000	1.0000	0.0000	0.0000	0.0000	0.0000	0.0000	0.0000
H <sub>2</sub> O	0.0000	1.0000	0.0000	1.0000	0.1763	0.1762	0.1762	0.1235	0.1235
Hydrogen	0.0000	0.0000	0.0000	0.0000	0.4708	0.4710	0.4710	0.5011	0.5011
CO <sub>2</sub>	0.0000	0.0000	0.0000	0.0000	0.2645	0.2646	0.2646	0.2815	0.2815
CO	0.0000	0.0000	0.0000	0.0000	0.0003	0.0002	0.0002	0.0002	0.0002
Methane	0.0000	0.0000	0.0000	0.0000	0.0880	0.0880	0.0880	0.0937	0.0937
DEAmine	0.0000	0.0000	0.0000	0.0000	0.0000	0.0000	0.0000	0.0000	0.0000
Stream	Make Up DEA	20c	16	17	Product	19	Hydrogen	Methane	Flue Gas
Vapor fraction	0.0000	0.0000	0.0000	0.0000	1.0000	0.0000	1.0000	0.9909	0.9971
Temperature (C)	25	25	25	40	41	93	30	30	71
Pressure (kPa)	100	100	100	270	250	250	2500	2500	100
Molar flow (kgmole/h)	0.02	25.34	25.36	25.36	5.26	28.55	4.19	1.07	3.21
Mass flow (kg/h)	1.66	2384.88	2386.54	2386.54	31.30	2500.06	8.45	22.85	113.86
Heat flow (MJ/h)	−8	−11654	−11662	−11572	−148	−12632	1	−150	−1097
Component	Mole Fraction								
Glycerol	0.0000	0.0000	0.0000	0.0000	0.0000	0.0000	0.0000	0.0000	0.0000
H <sub>2</sub> O	0.1500	0.1265	0.1266	0.1266	0.0022	0.1486	0.0000	0.0107	0.3277
Hydrogen	0.0000	0.0000	0.0000	0.0000	0.8048	0.0000	1.0000	0.0396	0.0002
CO <sub>2</sub>	0.0000	0.0000	0.0000	0.0000	0.0424	0.0755	0.0000	0.2088	0.6718
CO	0.0000	0.0000	0.0000	0.0000	0.0003	0.0000	0.0000	0.0016	0.0000
Methane	0.0000	0.0000	0.0000	0.0000	0.1502	0.0000	0.0000	0.7392	0.0003
DEAmine	0.8500	0.8735	0.8734	0.8734	0.0000	0.7758	0.0000	0.0000	0.0000

Glycerol steam reforming was simulated with the following operating conditions: reaction temperatures of 400–750 °C and a steam-to-glycerol molar ratio of 0.5–10. The effect of the steam-to-glycerol ratio on product composition is shown in Figure 3. In steam-deficient environments, the gas products were dominated by CO<sub>2</sub> and CH<sub>4</sub>. As the ratio of steam to glycerol increases, the hydrogen fraction in the product stream increases exponentially, reaching a maximum ratio of 4.5. As the ratio continued to increase, the number of unreacted steams increased and the hydrogen fraction decreased simultaneously. From the case study, it can be concluded that the steam-to-glycerol ratio should be around 4.5 to achieve the optimum result.

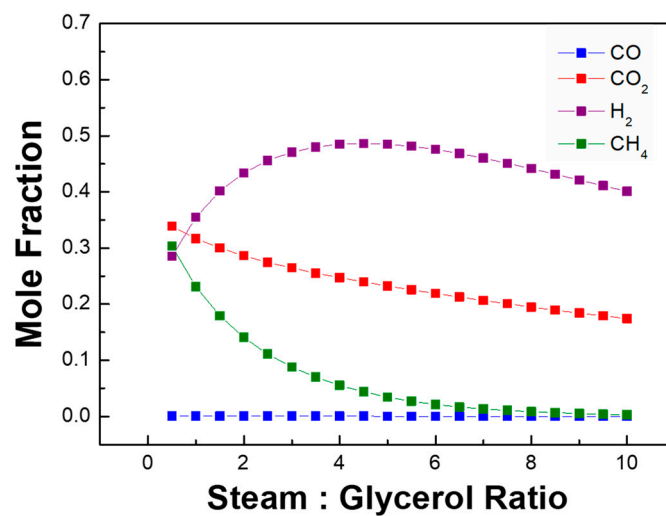


Figure 3. Effect of steam-to-glycerol ratio on product composition.

The effect of reaction temperature on the composition of the produced gas was also simulated, as shown in Figure 4. At the lowest simulation temperature, the hydrogen fraction is very low, and the process is deemed inefficient. As the temperature continued to rise, the hydrogen composition increased exponentially and dominated the product stream at the highest simulated temperature. The steam reforming reaction is endothermic, and high temperatures are preferred. However, higher reaction temperatures are economically undesirable [42].

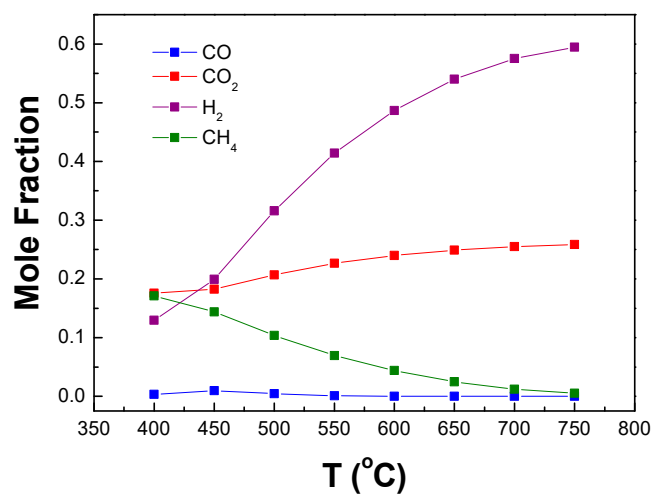


Figure 4. Effect of reaction temperature on product composition.

The next parameters to evaluate are hydrogen yield and selectivity. In the reaction process, high yield and selectivity for the desired products are preferable. Simulated data for hydrogen yield and selectivity at different reaction temperatures are shown in Figures 5 and 6, respectively. Both parameters showed similar trends. As the temperature rises, the hydrogen yield and selectivity increase significantly. Hydrogen yield and selectivity of 96.68% and 98.1%, respectively, were achieved at the maximum simulated temperature.

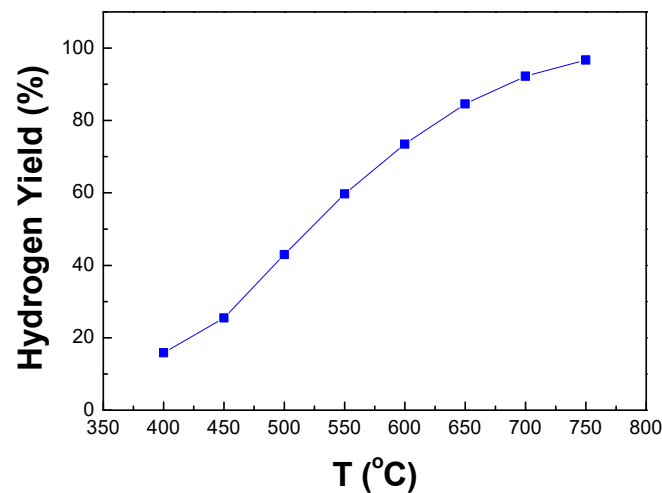


Figure 5. Effect of reaction temperature on hydrogen yield.

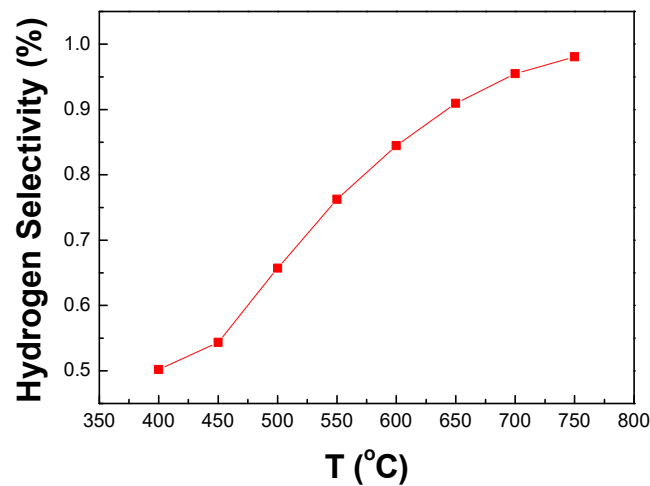


Figure 6. Effect of reaction temperature on selectivity of hydrogen.

### 3.3. Economic Analysis

As an initial consideration to further investigate the feasibility of the simulated process, a simple economic analysis is required. The economic analysis was carried out via the Aspen process economic analyzer (APEA) to calculate total capital and production costs. External data based on the average market price of CSO, biodiesel, and hydrogen were used for the rough revenue estimation. The projected annual expenditures and revenues are summarized in Table 10.

Table 10. Economic analysis results of an integrated biodiesel and hydrogen production from cottonseed oil.

Parameter	Value
Biodiesel production capacity (TPY)	8000
Hydrogen production (TPY)	70
Total capital cost (million USD)	5.8
Production cost (million USD/year)	0.9
Raw materials cost (million USD/year)	6.5
Revenue (million USD/year)	7.8

From the data reported in Table 10, the payback period (PBP), rate of return on investment (ROI), and internal rate of return (IRR) were calculated using Equations (3)–(5),

respectively, with supplementary assumptions of 11% interest rate ( $i$ ), 8-year project time ( $t$ ), and operation of the plant, which starts at the beginning of year 3. ROI does not take into account the time value of money. Meanwhile, IRR takes into account the time value of money and calculates the annual growth rate. The projected net present value (NPV) of the simulated processes is illustrated in Figure 7. As summarized in Table 11, the calculated results demonstrate that the integrated process of biodiesel and hydrogen production from CSO in small capacity has quite excellent investment criteria.

$$\text{PBP} = \frac{\text{Initial Investment} - \text{Opening Cumulative Cash Flow}}{\text{Closing Cumulative Cash Flow} - \text{Opening Cumulative Cash Flow}} \quad (11)$$

$$\text{ROI} = \frac{\text{Average net annual profit}}{\text{Fixed Capital Investment}} \quad (12)$$

$$\text{IRR} = i_a + \frac{\text{NPV}_a}{\text{NPV}_a - \text{NPV}_b} (i_b - i_a) \quad (13)$$

where  $i_a$  = lower discount rate chosen,  $i_b$  = higher discount rate chosen,  $\text{NPV}_a$  = net present value at  $i_a$ , and  $\text{NPV}_b$  = net present value at  $i_b$

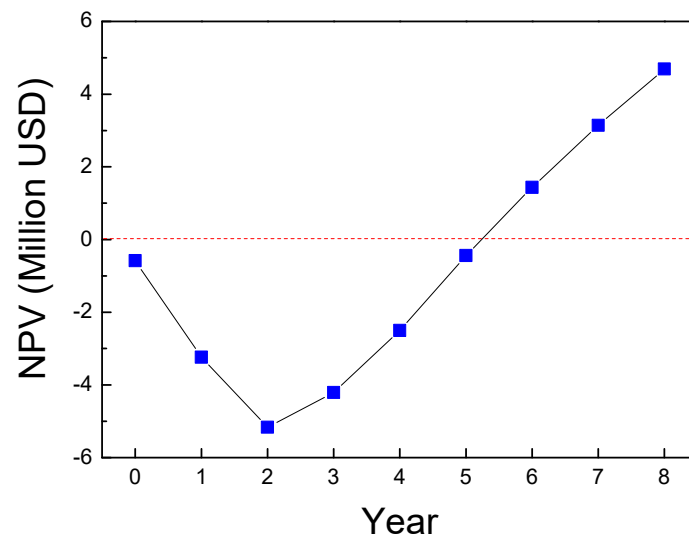


**Figure 7.** Projected net present value (NPV) of an integrated biodiesel and hydrogen production from cottonseed oil.

**Table 11.** Summary of investment criteria of integrated biodiesel and hydrogen production from cottonseed oil.

Parameter	Value
PBP	5.76
ROI	36%
IRR	28%

A sensitivity analysis was conducted to examine the impact of production variables such as biodiesel selling price and production capacity on gross margin. Input variable sensitivity limits are set at  $-50\%$  and  $+50\%$  of the base case. Figure 8 shows the results of the sensitivity analysis. There is a steep slope in production capacity compared to the price of biodiesel production. It can be concluded that production capacity has a greater impact on gross margins than biodiesel pricing.

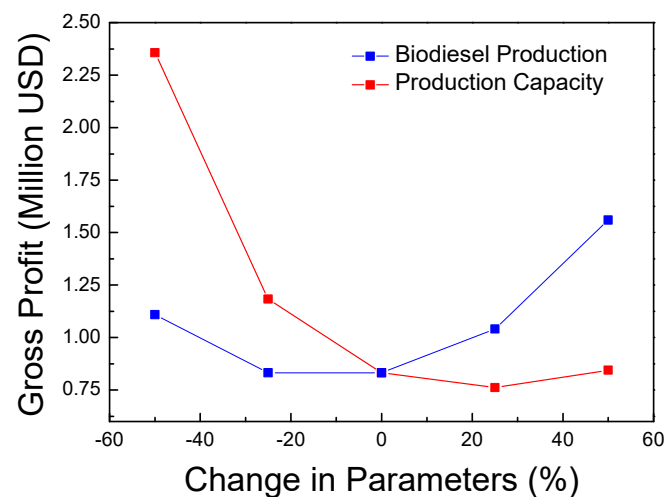


**Figure 8.** Sensitivity analysis of gross profit of integrated biodiesel and hydrogen production from cottonseed oil.

#### 4. Conclusions

This study aims to simulate an integrated process of biodiesel production from CSO and hydrogen production from glycerol, which is the by-product of the main process. In the initial process, CSO is converted to biodiesel via the transesterification process. In addition, since glycerol is a by-product in the initial stage, it is then utilized as the raw material in the following process. The second reaction involves four reactions in the main reactor: steam reforming, glycerol decomposition, water–gas shift, and methanation.

The optimum steam-to-glycerol molar ratio is 4.5, and the higher the reaction temperature, the higher the proportion of hydrogen in the gas stream, leading to higher hydrogen yield and selectivity. However, the energy consumption of this process needs to be further studied, as more energy must be supplied at higher temperatures. A simple economic analysis of the integrated process showed that this process is economically viable.

**Author Contributions:** Conceptualization, D.A.T., A.Z.A. and R.P.P.; methodology, D.A.T. and A.Z.A.; software, D.A.T., F.D.P. and A.S.H.; validation, D.A.T., A.Z.A. and F.D.P.; formal analysis, D.A.T.; investigation, D.A.T.; resources, D.A.T. and A.Z.A.; data curation, D.A.T.; writing—original draft preparation, D.A.T.; writing—review and editing, D.A.T., A.Z.A., R.P.P., F.D.P., A.S.H. and M.I.P.; visualization, D.A.T., F.D.P. and A.S.H.; supervision, A.Z.A.; project administration, D.A.T. and A.Z.A.; funding acquisition, D.A.T., A.Z.A. and R.P.P. All authors have read and agreed to the published version of the manuscript.

**Funding:** This research received no external funding.

**Institutional Review Board Statement:** Not applicable.

**Informed Consent Statement:** Not applicable.

**Data Availability Statement:** Not applicable.

**Acknowledgments:** The authors thank Institut Teknologi Bandung (ITB) and Politeknik Negeri Bandung (POLBAN) for financial supports.

**Conflicts of Interest:** The authors declare no conflict of interest.

#### References

- Perera, F. Pollution from Fossil-Fuel Combustion is the Leading Environmental Threat to Global Pediatric Health and Equity: Solutions Exist. *Int. J. Environ. Res. Public Health* **2017**, *15*, 16. [[CrossRef](#)] [[PubMed](#)]
- Moser, B.R. Fuel property enhancement of biodiesel fuels from common and alternative feedstocks via complementary blending. *Renew. Energy* **2016**, *85*, 819–825. [[CrossRef](#)]
- Shreyash, N.; Sonker, M.; Bajpai, S.; Tiwary, S.K.; Khan, M.A.; Raj, S.; Sharma, T.; Biswas, S. The Review of Carbon Capture-Storage Technologies and Developing Fuel Cells for Enhancing Utilization. *Energies* **2021**, *14*, 4978. [[CrossRef](#)]

4. Chandran, D. Compatibility of diesel engine materials with biodiesel fuel. *Renew. Energy* **2020**, *147*, 89–99. [[CrossRef](#)]
5. Rathore, V.; Newalkar, B.L.; Badoni, R.P. Processing of vegetable oil for biofuel production through conventional and non-conventional routes. *Energy Sustain. Dev.* **2016**, *31*, 24–49. [[CrossRef](#)]
6. Toldrá-Reig, F.; Mora, L.; Toldrá, F. Trends in Biodiesel Production from Animal Fat Waste. *Appl. Sci.* **2020**, *10*, 3644. [[CrossRef](#)]
7. Vassilev, S.V.; Vassileva, C.G. Composition, properties and challenges of algae biomass for biofuel application: An overview. *Fuel* **2016**, *181*, 1–33. [[CrossRef](#)]
8. Mohammadshirazi, A.; Akram, A.; Rafiee, S.; Kalhor, E.B. Energy and cost analyses of biodiesel production from waste cooking oil. *Renew. Sustain. Energy Rev.* **2014**, *33*, 44–49. [[CrossRef](#)]
9. Onukwuli, D.O.; Emembolu, L.N.; Ude, C.N.; Aliozo, S.O.; Menkiti, M.C. Optimization of biodiesel production from refined cotton seed oil and its characterization. *Egypt. J. Pet.* **2017**, *26*, 103–110. [[CrossRef](#)]
10. Soosai, M.R.; Moorthy, I.M.G.; Varalakshmi, P.; Yonas, C.J. Integrated global optimization and process modelling for biodiesel production from non-edible silk-cotton seed oil by microwave-assisted transesterification with heterogeneous calcium oxide catalyst. *J. Clean. Prod.* **2022**, *367*, 132946. [[CrossRef](#)]
11. Trirahayu, D.A. Process simulation of propylene production from crude palm oil by hydrodeoxygenation and propane dehydrogenation. *J. Phys. Conf. Ser.* **2020**, *1450*, 012009. [[CrossRef](#)]
12. Trirahayu, D.A. Process simulation of glycerol production from corn oil via transesterification. *IOP Conf. Ser. Mater. Sci. Eng.* **2020**, *830*, 6–10. [[CrossRef](#)]
13. Trirahayu, D.A. Simulation of Rice Bran Oil Transesterification Process for Biodiesel Production. In *International Seminar of Science and Applied Technology*; Atlantis Press: Amsterdam, The Netherlands, 2020; Volume 198, pp. 384–387. [[CrossRef](#)]
14. Trirahayu, D.A. Process Simulation of Glycerol Conversion to Formic Acid Using Hydrothermal Oxidation. In *International Conference on Innovation in Science and Technology*; Atlantis Press: Amsterdam, The Netherlands, 2021; Volume 208, pp. 179–182.
15. Trirahayu, D.A.; Abidin, A.Z.; Putra, R.P.; Hidayat, A.S.; Safitri, E.; Perdana, M.I. Process Simulation and Design Considerations for Biodiesel Production from Rubber Seed Oil. *Fuels* **2022**, *3*, 563–579. [[CrossRef](#)]
16. Encinar, J.; Pardal, A.; Sánchez, N.; Nogales, S. Biodiesel by Transesterification of Rapeseed Oil Using Ultrasound: A Kinetic Study of Base-Catalysed Reactions. *Energies* **2018**, *11*, 2229. [[CrossRef](#)]
17. Lima, P.J.M.; da Silva, R.M.; Neto, C.A.C.G.; e Silva, N.C.G.; Souza, J.E.D.S.; Nunes, Y.L.; dos Santos, J.C.S. An overview on the conversion of glycerol to value-added industrial products via chemical and biochemical routes. *Biotechnol. Appl. Biochem.* **2022**, *69*, 2794–2818. [[CrossRef](#)]
18. Cormos, A.-M.; Cormos, C.-C. Techno-economic and environmental performances of glycerol reforming for hydrogen and power production with low carbon dioxide emissions. *Int. J. Hydrogen Energy* **2017**, *42*, 7798–7810. [[CrossRef](#)]
19. Li, H.; Zhang, Y.; Fu, P.; Wei, R.; Li, Z.; Dai, L.; Zhang, A. Chemical looping steam reforming of glycerol for hydrogen production over NiO-Fe<sub>2</sub>O<sub>3</sub>/Al<sub>2</sub>O<sub>3</sub> oxygen carriers. *RSC Adv.* **2022**, *12*, 24014–24025. [[CrossRef](#)]
20. Loy, A.C.M.; Samudrala, S.P.; Bhattacharya, S. Evaluation of Porous Honeycomb-Shaped CuO/CeO<sub>2</sub> Catalyst in Vapour Phase Glycerol Reforming for Sustainable Hydrogen Production. *Catalysts* **2022**, *12*, 941. [[CrossRef](#)]
21. Kuppasamy, M. Optimization and Production of Biodiesel from Cottonseed Oil and Neem Oil. 2016. Available online: <https://www.researchgate.net/publication/303792895> (accessed on 29 March 2023).
22. Shankar, A.A.; Pentapati, P.R.; Prasad, R.K. Biodiesel synthesis from cottonseed oil using homogeneous alkali catalyst and using heterogeneous multi walled carbon nanotubes: Characterization and blending studies. *Egypt. J. Pet.* **2017**, *26*, 125–133. [[CrossRef](#)]
23. Moawia, R.M.; Nasef, M.M.; Mohamed, N.H.; Ripin, A.; Farag, H. Production of Biodiesel from Cottonseed Oil over Aminated Flax Fibres Catalyst: Kinetic and Thermodynamic Behaviour and Biodiesel Properties. *Adv. Chem. Eng. Sci.* **2019**, *9*, 281–298. [[CrossRef](#)]
24. Djomdi; Leku, M.T.; Djoulde, D.; Delattre, C.; Michaud, P. Purification and Valorization of Waste Cotton Seed Oil as an Alternative Feedstock for Biodiesel Production. *Bioengineering* **2020**, *7*, 41. [[CrossRef](#)] [[PubMed](#)]
25. Yang, A.; Qi, M.; Wang, X.; Wang, S.; Sun, L.; Qi, D.; Zhu, L.; Duan, Y.; Gao, X.; Rajput, S.A.; et al. Refined cottonseed oil as a replacement for soybean oil in broiler diet. *Food Sci. Nutr.* **2019**, *7*, 1027–1034. [[CrossRef](#)] [[PubMed](#)]
26. Lee, D. Preparation of a sulfonated carbonaceous material from lignosulfonate and its usefulness as an esterification catalyst. *Molecules* **2013**, *18*, 8168–8180. [[CrossRef](#)] [[PubMed](#)]
27. Zaccheria, F.; Brini, S.; Psaro, R.; Scotti, N.; Ravasio, N. Esterification of acidic oils over a versatile amorphous solid catalyst. *ChemSusChem* **2009**, *2*, 535–537. [[CrossRef](#)] [[PubMed](#)]
28. Lin, L.; Ying, D.; Chaitep, S.; Vittayapadung, S. Biodiesel production from crude rice bran oil and properties as fuel. *Appl. Energy* **2009**, *86*, 681–688. [[CrossRef](#)]
29. Mazaheri, H.; Ong, H.C.; Masjuki, H.H.; Amini, Z.; Harrison, M.D.; Wang, C.-T.; Kusumo, F.; Alwi, A. Rice bran oil based biodiesel production using calcium oxide catalyst derived from *Chicoreus brunneus* shell. *Energy* **2018**, *144*, 10–19. [[CrossRef](#)]
30. Evangelista, J.P.C.; Chellappa, T.; Coriolano, A.C.F.; Fernandes, V.J.; Souza, L.D.; Araujo, A.S. Synthesis of alumina impregnated with potassium iodide catalyst for biodiesel production from rice bran oil. *Fuel Process. Technol.* **2012**, *104*, 90–95. [[CrossRef](#)]
31. Lakshmi, S.B.A.V.S.; Pillai, N.S.; Mohamed, M.S.B.K.; Narayanan, A. Biodiesel production from rubber seed oil using calcined eggshells impregnated with Al<sub>2</sub>O<sub>3</sub> as heterogeneous catalyst: A comparative study of RSM and ANN optimization. *Braz. J. Chem. Eng.* **2020**, *37*, 351–368. [[CrossRef](#)]

32. Bharadwaj, A.V.S.L.S.; Singh, M.; Niju, S.; Begum, K.M.M.S.; Anantharaman, N. Biodiesel production from rubber seed oil using calcium oxide derived from eggshell as catalyst-optimization and modeling studies. *Green Process. Synth.* **2019**, *8*, 430–442. [[CrossRef](#)]
33. Zamberi, M.M.; Ani, F.N. Biodiesel production from high FFA rubber seed oil using waste cockles. *ARPN J. Eng. Appl. Sci.* **2016**, *11*, 7782–7787.
34. Jariah, N.F.; Hassan, M.A.; Taufiq-Yap, Y.H.; Roslan, A.M. Technological advancement for efficiency enhancement of biodiesel and residual glycerol refining: A mini review. *Processes* **2021**, *9*, 1198. [[CrossRef](#)]
35. Trisnaliani, L.; Zaki, A. Separation of Glycerol from Biodiesel Oil Products Using High Voltage Electrolysis Method. *Indones. J. Fundam. Appl. Chem.* **2018**, *3*, 7–11. [[CrossRef](#)]
36. Dhar, B.R.; Kirtania, K. Excess Methanol Recovery in Biodiesel Production Process Using a Distillation Column: A Simulation Study. *Chem. Eng. Res. Bull.* **2009**, *13*, 55–60. [[CrossRef](#)]
37. Baroutian, S.; Aroua, M.K.; Raman, A.A.A.; Sulaiman, N.M.N. Methanol recovery during transesterification of palm oil in a TiO<sub>2</sub>/Al<sub>2</sub>O<sub>3</sub> membrane reactor: Experimental study and neural network modeling. *Sep. Purif. Technol.* **2010**, *76*, 58–63. [[CrossRef](#)]
38. Saleh, J.; Tremblay, A.Y.; Dubé, M.A. Glycerol removal from biodiesel using membrane separation technology. *Fuel* **2010**, *89*, 2260–2266. [[CrossRef](#)]
39. Hajilary, N.; Rezakazemi, M.; Shirazian, S. Biofuel types and membrane separation. *Environ. Chem. Lett.* **2019**, *17*, 1–18. [[CrossRef](#)]
40. Alhassan, Y.; Kumar, N.; Bugaje, I.M.; Pali, H.S.; Kathkar, P. Co-solvents transesterification of cotton seed oil into biodiesel: Effects of reaction conditions on quality of fatty acids methyl esters. *Energy Convers. Manag.* **2014**, *84*, 640–648. [[CrossRef](#)]
41. Augustine, A.; Marimuthu, L.; Muthusamy, S. Performance and Evaluation of DI Diesel Engine by using Preheated Cottonseed Oil Methyl Ester. *Procedia Eng.* **2012**, *38*, 779–790. [[CrossRef](#)]
42. Carrero, A.; Calles, J.; García-Moreno, L.; Vizcaíno, A. Production of Renewable Hydrogen from Glycerol Steam Reforming over Bimetallic Ni-(Cu,Co,Cr) Catalysts Supported on SBA-15 Silica. *Catalysts* **2017**, *7*, 55. [[CrossRef](#)]

**Disclaimer/Publisher's Note:** The statements, opinions and data contained in all publications are solely those of the individual author(s) and contributor(s) and not of MDPI and/or the editor(s). MDPI and/or the editor(s) disclaim responsibility for any injury to people or property resulting from any ideas, methods, instructions or products referred to in the content.